

Proceedings of the European Conference "Physics of Magnetism '99", Poznań 1999

STRAINED TETRAGONAL BAIN PATHS IN Fe₃Pt INVAR

M. PUGACZOWA-MICHALSKA AND S. LIPÍŃSKI

Institute of Molecular Physics, Polish Academy of Sciences
Smoluchowskiego 17, 60-179 Poznań, Poland

Employing the LMTO-ASA method we calculated the total energy variation of Fe₃Pt along the tetragonal distortion path connecting fcc and bcc structures for isotropic biaxial path and uniaxially strained path and compare the results with energies for the unstrained path.

PACS numbers: 75.50.Bb, 81.30.Kf

1. Introduction

Iron-platinum alloys near the stoichiometric composition Fe₃Pt exhibit very small or even negative thermal expansion below the Curie temperature, which is known as the invar effect [1] (ordered Fe₃Pt $T_C = 510$ K, disordered Fe₃Pt $T_C = 375$ K). It is generally agreed that the invar properties are due to the closeness of an interplay between the ferromagnetic high-spin state (HS) with a large volume and non-magnetic (NM) or low-spin states (LS) with smaller volumes. In our previous paper we stressed an importance of additional excitations lying in the thermal range — magnetodistortive fluctuations [2]. Their role in breaking the symmetry of the lattice modes was discussed in Ref. [3]. In addition to the local distortions also the large-strain homogeneous lattice distortions are of importance for Fe₃Pt. Iron-platinum invar undergoes a martensitic phase transformation from fcc to bcc phase as the temperature is lowered, which is correlated with a dramatic softening of the $c_{11} - c_{12}$ shear elastic constant [4]. The martensitic transition manifests also in the occurrence of an unexpected "central" phonon peak around $\hbar\omega = 0$ in the [110] direction [4], extremely large value of the Grüneisen parameter and the pressure dependence of transverse acoustic phonon modes [5], as well as the anomalies in the susceptibility, specific heat [6] and magnetic anisotropy [7].

In the present paper we discuss the simplest homogeneous fcc-bcc lattice transformation — tetragonal Bain deformation. We consider the zero pressure path and compare the results with the two, physically realisable strained tetragonal paths: the epitaxial Bain path (EPB) and the uniaxial Bain path (UPB). The former is produced by isotropic stress in the (001) plane of tetragonal phases accompanied by vanishing stress perpendicular to the plane. Epitaxy provides a valuable means of stabilising metastable phases and of putting phases under very

large strains, both tensile and compressive in the plane of epitaxy. In UPB the uniaxial stress is applied to a tetragonal state along the [001] axis accompanied by zero stress in the (001) plane.

2. Computational method

We use a tight-binding linear muffin-tin orbital (LMTO) method in the atomic sphere approximation (ASA) [8] with the local exchange-correlation potential of Barth and Hedin [9]. The combined correction terms which minimise the ASA errors were included. As the convergence criterion of the energy on successive iterations, 0.02 mRy was used. The calculations were performed for 286 k points per irreducible wedge of fcc and bcc structures ($\frac{1}{48}$ of Brillouin zone, B.Z.) and 726 for tetragonally distorted systems ($\frac{1}{16}$ of B.Z.). The radii of the atomic spheres of platinum and iron were allowed to change slightly with the distortion and with the change of volume. Every time the atomic radii ratio was chosen by the requirement of the minimal charge transfer between the atomic spheres.

3. Results

Figure 1 shows the results for the total energy when we follow Bain path from fcc ($c/a = 1$) to bcc structure ($c/a = 0.7071$). The squares represent the minimal energies for the unstrained path ($\partial E/\partial V = 0$, $\partial^2 E/\partial V^2 > 0$). The bcc structure is lower in energy than fcc which is in agreement with the experimental observation of bcc phase as the low temperature state ($\Delta E = 0.58$ mRy/atom). Surprisingly high is the calculated lattice deformation barrier (≈ 2.6 mRy) suggesting high interfacial energy of martensitic nuclei. The EPB is calculated with a being fixed and c adjusts to minimise $E(c)$ and thus making the out-of-plane stress to vanish. Conversely, the UPB calculation fixes c and lets a adjust to minimise $E(a)$, making the in-plane stress to vanish. The strained paths have higher energy barriers than the unstrained path. The increase mainly results from the differences in the volumes of elementary cells. Whereas for the unstrained and EPB paths the volumes are very close to each other in the range of barrier, for UPB system the Wigner-Seitz (WS) radius is larger by 0.4%. Our energy estimations are only very crude due to the shortcomings of ASA in the strong deformation region. Another important oversimplification of our calculations is the rigid lattice approximation, which neglects the zero-point energy corrections. For the narrow deformation region $0.82 < c/a < 0.86$ the self-consistent LMTO equations become unstable and no conclusion on the shape of energy curves in this range is possible.

The pressure makes Fe_3Pt more stable against the martensitic transformation [5]. We performed the energy calculations for different hydrostatic pressure paths (equal in-plane and out-of-plane stress components) for distortions close to fcc and bcc structures and in the range of barrier. The results are summarised in Fig. 2. The relative decrease in Wigner-Seitz radius $\Delta R_{\text{WS}}(p)/R_{\text{WS}}(0)$ by one percent results in the increase in barrier energy by thirty percent. The calculated electronic pressure ($-\partial E/\partial V$), $p_e(R_{\text{WS}} = 0.99R_{\text{WS}}(0)) = 4.1$ GPa. For comparison, the corresponding pressure derived from the measured changes of the lattice parameters for the slightly different composition $\text{Fe}_{72}\text{Pt}_{28}$ is 5.7 GPa [10]. The

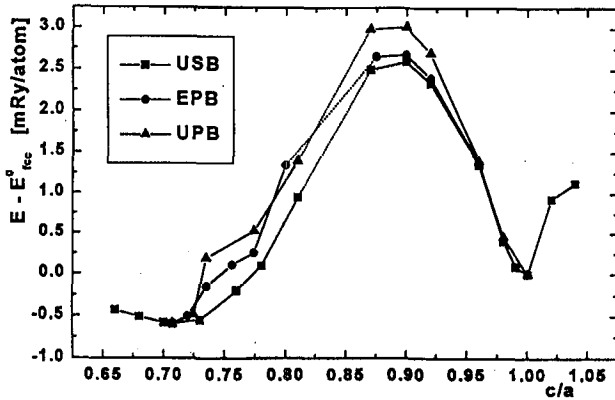


Fig. 1. The energy of Fe_3Pt along the unstrained (USB), epitaxial (EPB), and uniaxial (UPB) Bain paths. Dotted lines are used to mark the regions of numerical instabilities.

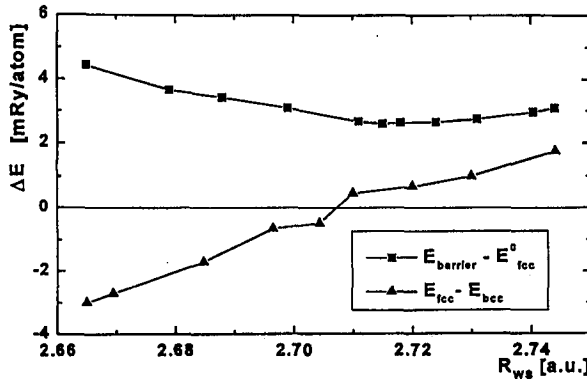


Fig. 2. The energy difference of fcc and bcc states and the lattice deformation barrier vs. Wigner-Seitz radius.

calculated bcc equilibrium radius is 2.733 a.u. For $R_{WS} = 2.707$ the fcc (HS) state becomes the ground state. The central role in stabilising the fcc structure is played by $dd\sigma$ bonds formed by t_{2g} orbitals pointing towards the twelve nearest neighbours. The t_{2g} subbands are most strongly affected by distortions and it is the main reason for the starting increase in energy with the decrease in c/a (Fig. 1). A compression of fcc system causes a broadening of the subbands and their repopulation. For $R_{WS} = 2.662$ a.u. the Fermi level shifts from the position slightly above the majority band edge into the position just below and a transition into the NM state results. The pictures of the DOS for different distortions are given in Ref. [2].

An open question is what stabilises the high-temperature fcc phase at zero pressure. The difference of the electronic specific heats of both phases is much too small and the corresponding entropy excess is out of importance for the bcc-fcc transition. The calculated DOS at the Fermi level yield 82 states/Ry and 50 states/Ry per formula unit for the fcc and bcc states, respectively. A plau-

sible driving force of martensitic transition might be the extra entropy associated with $HS \rightleftharpoons LS$ magnetovolume and magnetodistortive fluctuations in the fcc phase [1, 2]. The vibronic part of the entropy might be also of importance, but the experimentally observed hardening of some phonon branches with transition to fcc phase [4] suggests the decrease in entropy. The hardening effect is partly related to the increase in the coordination number and a small decrease in volume with transition, but mainly results from magnetoelastic coupling. Our preliminary estimations of tetragonal shear constants show that they do not differ significantly for bcc and fcc (HS) states but a corresponding value for NM fcc state is much larger. Unfortunately, the ASA restrictions and an insufficient accuracy of our total energy calculations do not allow us to obtain the precise values of elastic constants.

References

- [1] E.F. Wassermann, in: *Ferromagnetic Materials*, Vol. 5, Eds. K.H.J. Buschow, E.P. Wohlfarth, North-Holland, Amsterdam 1990.
- [2] S. Lipiński, M. Pugaczowa-Michalska, *Physica B* **269**, 227 (1999).
- [3] S. Lipiński, K.U. Neumann, K.R.A. Ziebeck, *J. Phys., Condens. Matter* **6**, 1527 (1994).
- [4] K. Tajima, Y. Endoh, Y. Ishikawa, W.G. Stirling, *Phys. Rev. Lett.* **37**, 519 (1976).
- [5] M. Schoerber-Böhnig, S. Klotz, J.M. Besson, E. Burkel, M. Braden, I. Pintschovius, *Europhys. Lett.* **33**, 679 (1996).
- [6] E.F. Wassermann, N. Schubert, J. Kästner, B. Rellinghaus, *J. Magn. Magn. Mater.* **140-144**, 229 (1995).
- [7] A. Sakuma, *J. Phys. Soc. Jpn.* **64**, 4317 (1995).
- [8] O.K. Andersen, *Phys. Rev. B* **12**, 3060 (1975).
- [9] U. von Barth, L. Hedin, *J. Phys. C* **5**, 1629 (1972).
- [10] G. Oomi, N. Mori, *J. Phys. Soc. Jpn.* **50**, 2917 (1981).